Electronic Supplementary Material (ESI) for Chemical Communications.
This journal is © The Royal Society of Chemistry 2015

Supporting information

The Opposite Gating Behaviors of Solid-State Nanochannels Modified with Long and Short Polymer Chains**

Juntao Zhang,[a,b,c] Nannan Liu,[a] Benmei Wei,[a] Xiaowen Ou,[a] Xuemei Xu,[a] Xiaoding Lou[a] and Fan Xia*[,a,b]

[a]Key Laboratory for Large-Format Battery Materials and System, Ministry of Education, School of Chemistry and Chemical Engineering, Huazhong University of Science and Technology, Wuhan, Hubei 430074, P. R. China

[b]National Engineering Research Center for Nanomedicine, College of Life Science and Technology, Huazhong University of Science and Technology, Wuhan, Hubei 430074, P. R. China

[c] School of Chemical and Environmental Engineering, Wuhan Polytechnic University, Wuhan, Hubei 430023, P. R. China

* To whom correspondence should be addressed: xiafan@hust.edu.cn .

Table of the contents

1. Materials.

Anodic aluminum oxide (AAO) membranes were purchased from Puyuan Nano (Hefei, China), the pore diameters of the AAO we used in this work were about 40–70 nm, and the thickness of the membrane is about 100 μm. 3-Aminopropyltrimethoxysilane (APTMS), 2-Bromoisobutyryl bromide (BIBB), N-Isopropylacrylamide (NIPAAm), 1,1,4,7,7-Pentamethyl-diethylenetriamine (PMDETA), and Copper(I) bromide were obtained from Sigma-Aldrich Co. (St. Louis, MO, USA). (m-Acrylamidophenyl)boronic acid was purchased from Sukailu reagent Co. (Suzhou, China). Chemical reagents were all used as received. The NIPAAm was recrystallized from a mixture of toluene and n-hexane (1:3, v/v) before use. All other chemicals used in this work were analytical grade and used as received. All solutions were prepared in MilliQ water (18.2 MΩ).

2. Chemical Modification of AAO Nanochannels.

The AAO membranes were firstly cleaned with ultrasound treatment in a mixture of 1 mL ethanol and purified water (1:1, v/v) for 5 minutes. Afterwards, the membranes were immersed in 1 mL 5% HCl solution for 20-30 seconds. Then they were washed with H_2O and dried under a flow of nitrogen gas. After that, the membranes were immersed into 800 μL 5 % acetone solution of APTMS, ultrasonic for 5 min to make sure that the solution can fill the nanochannels sufficiently. The reaction was carried out for 10 h at room temperature to obtain chemically bonded $–NH_2$ groups.[1,2] The membranes were thoroughly washed in acetone and dried under nitrogen flow, and then the membranes were put into 792 μL of dry DCM containing dry Et_3N (8 μL). Afterwards, 8 μL BIBB was added into the solvent with an ice bath and untrasonic for 5 min, then the reaction was left overnight at room temperature. The resultant membrane with –Br groups was then cleaned with acetone and ethanol, and dried by a flow of nitrogen gas. Polymerization of NIPAAM-*co*-PBA was achieved by immersing the AAO substrates with initiator in a degassed solution of NIPAAm (84.8 mg) and PBA (7.2 mg) (5 mol% of PBA against NIPAAm) in a 1:1 (v/v) mixture of H_2O and CH_3OH (800 μL) containing CuBr (2.6 mg) and pentamethyl diethylene triamine (PMDETA) (11.2 μL) for 1 h or 10 min at 60 ^oC.[3] After that, the AAO membranes were washed thoroughly with pure H_2O and stored in H_2O at room temperature.

Ionic transport properties of the nanochannel system before and after chemical modification have been examined by corresponding Current-Voltage (*I*–*V*) curves

measured using 0.1 M KCl electrolyte solution at pH 7 in both half–cells. Figure S1 shows *I–V* properties of the nanochannel system before and after chemical modification, and also demonstrates that the polymer chain length can be controlled by varying polymerization time. After 10 min polymerization, a nearly 60% decrease in the conductance of the nanochannel system is found. Along the reaction time increasing to 60 min, the ion conductance of the nanochannel system decreases further to 6%. The results showed here presents strong evidence for the successful modification of the copolymers into the nanochannel. The successful modification can also be characterized by X-ray photoelectron spectroscopy (XPS) analysis (Tables S1 and S2, Supporting Information) and contact angle measurements (Figure S2, Supporting Information).

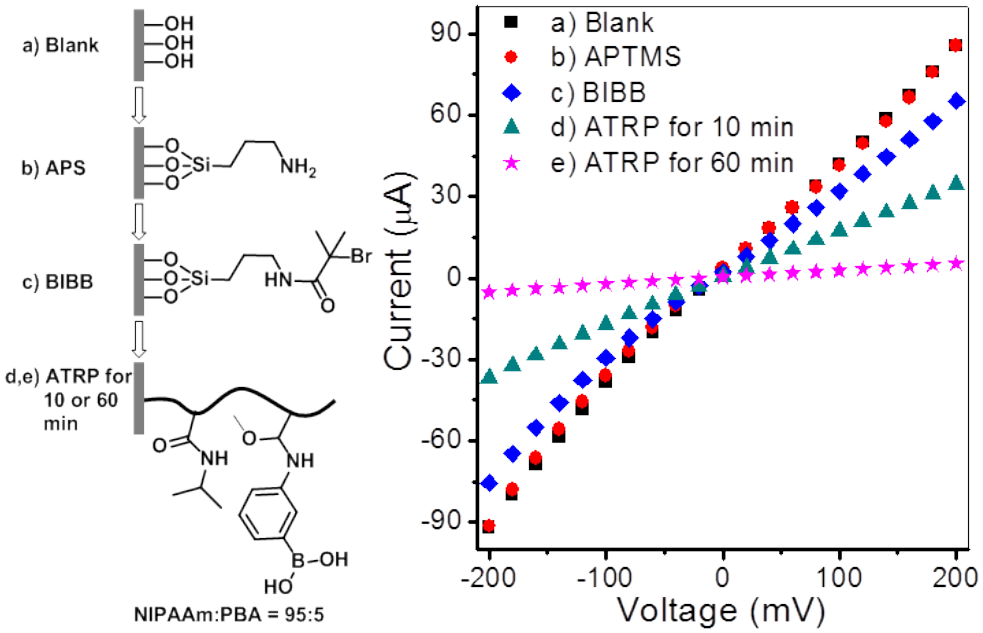

Figure S1. The modification processes and the corresponding *I*–*V* curves. a) Pristine AAO nanochannel (square, blank). b) After the conversion of the surface hydroxyl group into terminal amino groups (circle, red). c) After the conversion of the amino groups into ATRP initiator (diamond, blue). d,e) After the ATRP for 10 min (triangle, dark cyan, d) and 60 min (star, magenta, e).

3. Current–Voltage Recordings.

The nanochannel membrane was mounted between two halves of a conductivity cell; and each half-cell was filled with 0.1 M potassium chloride solution. The pH of the electrolyte was adjusted with 1 M HCl or KOH solutions. Ag/AgCl electrodes were settled in each half-cell to apply desired transmembrane potential and to measure the resulting ionic current. The current was recorded with a Keithley 6487 picoammeter/voltage source (Keithley Instruments). The temperature of the electrolyte solution inside the cell was detected with a commercial thermodetector and was controlled via a heating apparatus outside the cell.

4. X-ray photoelectron spectra characterization.

X-ray photoelectron spectra (XPS) data were obtained with an ESCALab220i-XL electron spectrometer from VG Scientific using 300W Al Kα radiation. All peaks were referenced to C 1s (CHx) at 284.8 eV in the deconvoluted high resolution C 1s spectra, and the analysis software used was provided by the manufacturer. Table S1 and S2 showed the XPS data from PI film before and after chemical modification, respectively. The changes of element content confirm the successful immobilization of copolymer on the surface of AAO film.

Table S1. The XPS data from AAO film before modification

Name	Start BE	Peak BE	End BE	Height CPS	FWHM eV	Area (P) CPS.eV	At. %
O 1s	538.2	532.0	526.2	75198.65	2.459	203392.4	80.39
C 1s	293.2	284.95	282.2	9909.59	1.447	16083.9	18.89
N 1s	405.2	399.69	396.2	596.12	1.547	1087.6	0.72

Table S2. The XPS data from AAO film after modification

Name	Start BE	Peak BE	End BE	Height CPS	FWHM eV	Area (P) CPS.eV	At. %
O 1s	538.45	532.23	526.45	30859.7	2.803	86739.3	80.08
C 1s	292.45	284.97	282.45	3209.1	1.871	6757.0	18.54
N 1s	403.45	399.54	395.45	842.83	1.292	888.0	1.37
B 1s	196.45	189.67	186.45	53.24	0.140	1.6	0.01

5. CA measurement of AAO membranes before and after modification.

Contact angles were measured using an OCA20 (DataPhysics, Germany) contact-angle system at ambient temperature and saturated humidity. The water droplet is 2 μL and the measurement was in five different locations of the membrane. As shown in Figure S2, CA of the naked plate AAO membrane is about 31° at 18 ^{o}C (Figure S2 a); the CA almost no change along with the temperature increasing to 43 ^{o}C (Figure S2 b). The CA decreases to about 9° after modified with copolymers at 18 ^{o}C (Figure S2 c); and the CA increases to about 26° when the temperature increased to 43 ^{o}C (Figure S2 d). It clearly indicated the modification is successful.

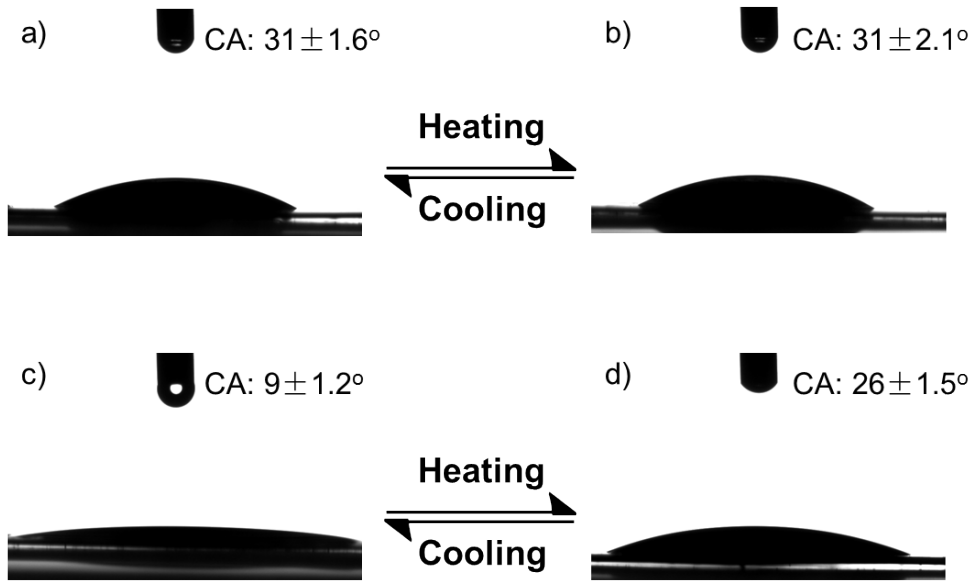

Figure S2. Photographs of water droplet on the AAO films. naked (a,b), modified with copolymers (c,d) at 18°C (a,c) and 43 °C (b,d).

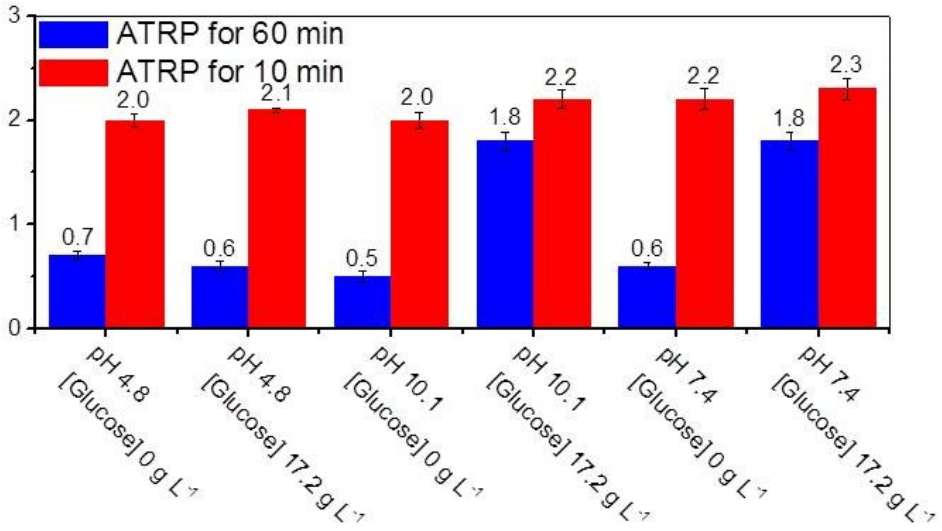

Figure S3. Current temperature gating ratios R_T (calculated as the current at 43 °C divided by the current at 18 °C measured at +2 V) of **NCS-60** and **NCS-10** under different pH and glucose concentration conditions.

As shown in Figure S3, we observed the remarkable difference of the temperature gating between the **NCS-60** and **NCS-10**. For **NCS-60**, two distinguishable types of temperature responses are manifested under different pH and glucose concentration. While the **NCS-10** shows a constant temperature response. When the pH is 4.8 without and with glucose, or the pH is 10.1 and 7.4 without glucose, the **NCS-60** shows a negative temperature gating behavior with R_T below 1. When the pH is 10.1 and 7.4 and the glucose concentration is 17.2 g L^{-1}, the **NCS-60** shows a positive temperature gating behavior with a R_T of 1.8 and 1.8, respectively. As a comparison, the **NCS-10** always shows positive temperature gating behavior with R_T around 2 under all conditions mentioned above. These results illustrate that the long and short polymer chains is very important for the gating performance of the nanochannel system. For the long copolymers modified **NCS-60**, its temperature gating behavior is controlled by the volume exclusion

principle and hydrophobic interaction cooperatively. In contrast, temperature gating behavior of the short copolymers modified **NCS-10** is only controlled by the volume exclusion principle.

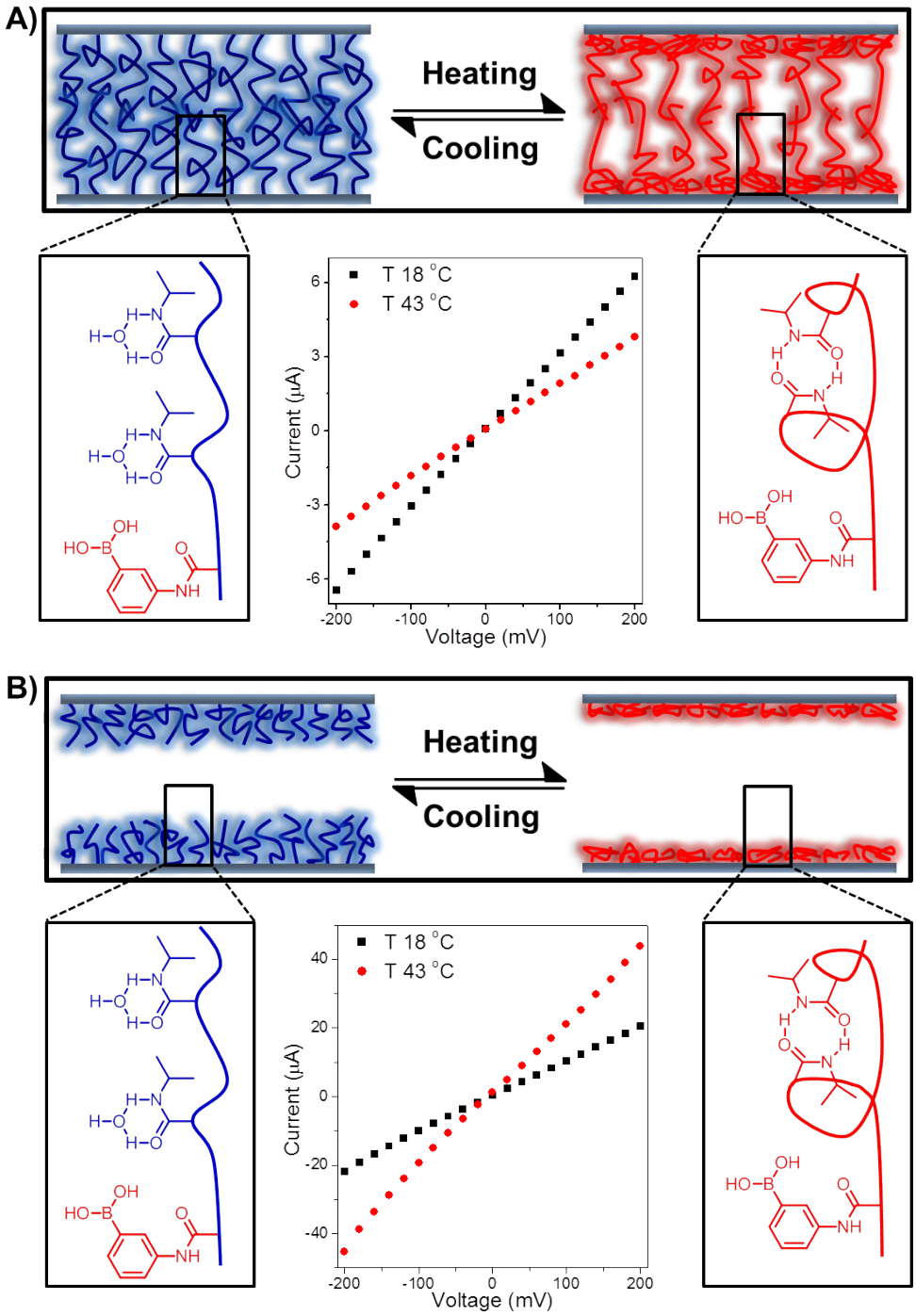

Figure S4. Temperature–responsive gating of **NCS-60** and **NCS-10** when the pH is 4.8 and glucose concentration is 17.2 g L^{-1}. a) Simplified illustration indicating the thick polymer layer morphology and hydrophilic/hydrophobic changes occurring in **NCS-60** upon variations of temperarure (top), and the corresponding conformation changes of the

copolymers on the inner surface of nanochannel (bottom left and right). *I-V* curves of this nanochannel system at 18 and 43 ^{o}C (bottom middle). b) Simplified illustration indicating the thin polymer layer morphology and hydrophilic/hydrophobic changes occurring in **NCS-10** upon variations of temperarure (top), and the corresponding conformation changes of the copolymers on the inner surface of nanochannel (bottom left and right). *I-V* curves of this nanochannel system at 18 and 43 ^{o}C (bottom middle).

When glucose concentration is 17.2 g L^{-1} and pH is 4.8 (Fig. S3). The ionic current of **NCS-60** decreases with a temperature gating ratio of 0.6 (negative gating behavior), along with the temperature increases from 18 ^{o}C to 43 ^{o}C (Fig. S3a). In contrast, the ionic current of **NCS-10** increases with a temperature gating ratio of 2.1 (positive gating behavior) in this process (Fig. S3b). The temperature responsive gating performance of **NCS-60** and **NCS-10** under this condition is consistent with which described in Figure 1C,D, because the neutral PBA moieties cannot form stable complex with glucose, the addition of glucose does not have influence on the hydrophilicity/hydrophobicity of copolymers. As a result, the observed opposite gating performances between **NCS-60** and **NCS-10** are also directly related to MLOP under this condition.

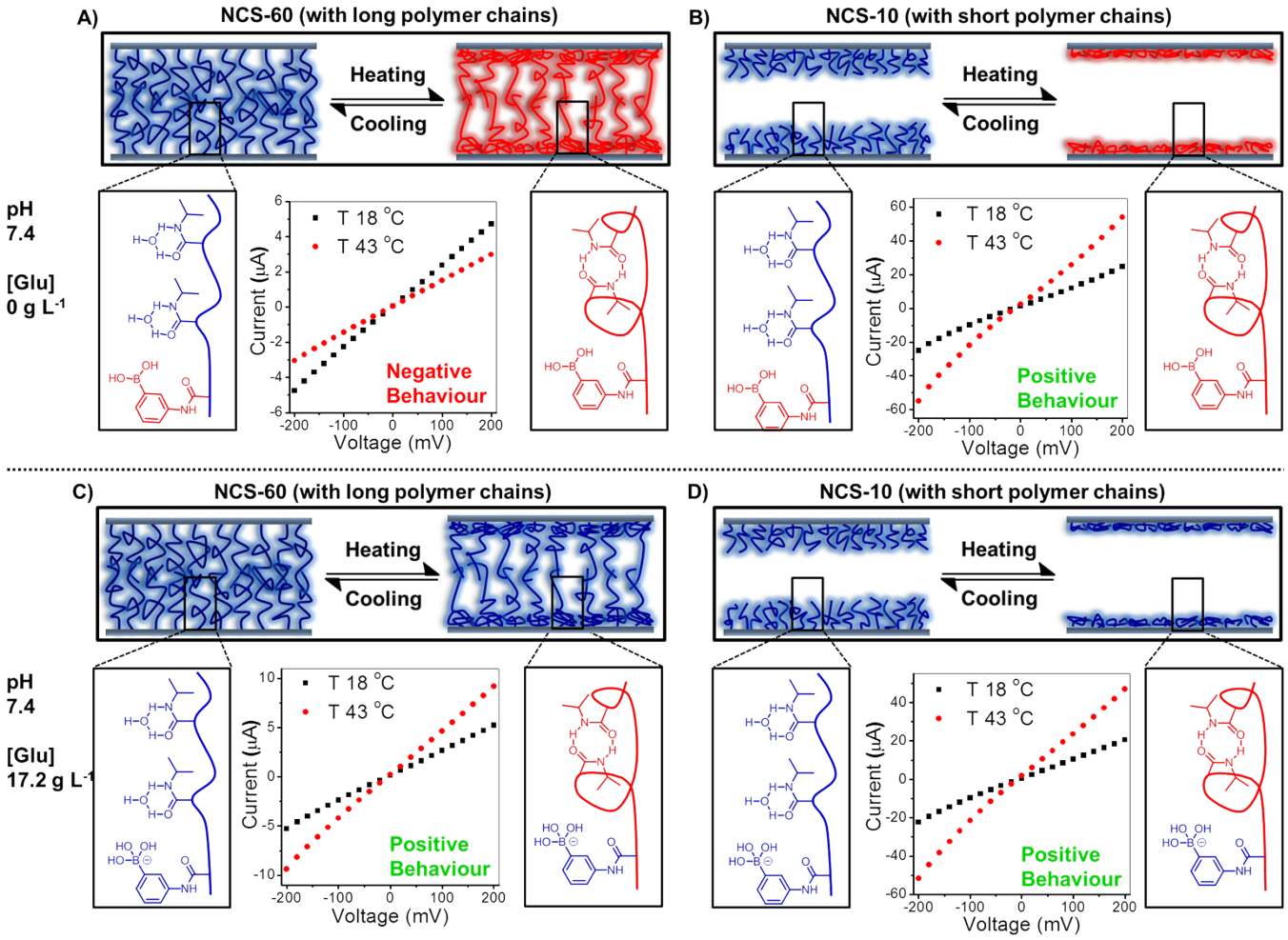

Figure S5. The influence of long and short polymer chains on the gating performances of nanochannel systems, when the pH is 7.4 and glucose concentration is 0 g L^{-1} (A,B) and the pH is 7.4 and glucose concentration is 17.2 g L^{-1} (C,D). Simplified illustration indicating the copolymer layer morphology and hydrophilic (indicated by the blue color)/hydrophobic (indicated by the red color) changes occurring in **NCS-60** and **NCS-10** upon variation of temperature. *I-V* curves of **NCS-60** (middle insets of A and C) and **NCS-10** (middle insets of B and D) at 18 and 43 °C, and the corresponding conformation changes of the copolymers on the inner surface of nanochannels (left and right insets).

In order to avoid the influence of the hydroxyl ions in the basic electrolyte solution. The experiments were also carried out under the physuoligal rang (pH 7.4). When the pH is 7.4

and the glucose concentration is 0 g L^{-1}, the ionic current of **NCS-60** decreases with a temperature gating ratio of 0.6 (Figure S3, Supporting Information) (negative gating behavior), along with the temperature increases from 18 ^{o}C to 43 ^{o}C (Figure S5A). As a comparison, the ionic current of **NCS-10** increases with a temperature gating ratio of 2.2 (Figure S3, Supporting Information) (positive gating behavior) in this process (Figure S5B). Then, the temperature gating behaviors of **NCS-60** and **NCS-10** is studied when the glucose concentration changes from 0 to 17.2 g L^{-1} (Figure S5C,D). Under this condition, **NCS-60** shows a positive temperature gating behavior with a gating ratio of 1.8 (Figure S3, Supporting Information), along with the temperature increases from 18 ^{o}C to 43 ^{o}C (Figure S5C), while the **NCS-10** shows a positive temperature gating behavior with a gating ratio of 2.3 (Figure S3, Supporting Information) (Figure S5D).

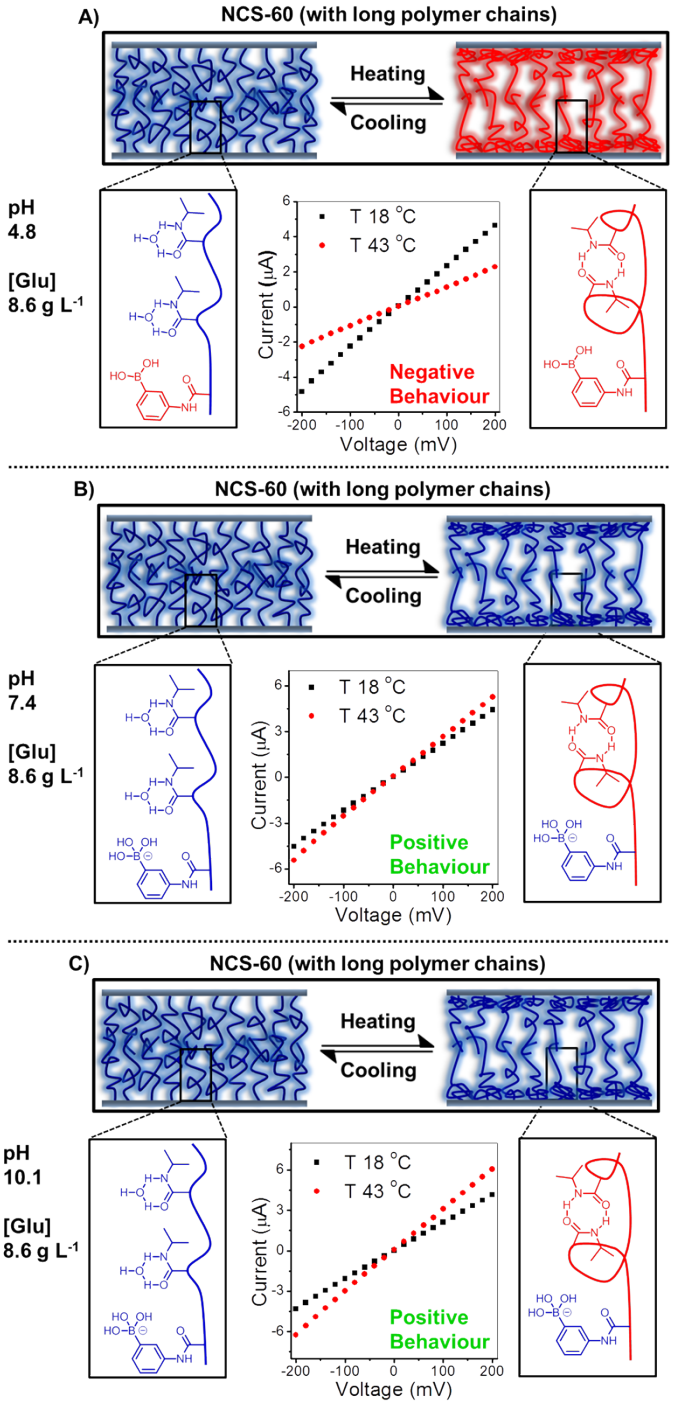

Figure S6. The gating performances of nanochannel systems modified with long polymer chains (**NCS-60**), when glucose concentration is 8.6 g L^{-1} and the pH is 4.8 (A), 7.4 (B), and 10.1 (C). Simplified illustration indicating the copolymer layer morphology and hydrophilic (indicated by the blue color)/hydrophobic (indicated by the red color) changes occurring in **NCS-60** upon variation of temperature. *I-V* curves of **NCS-60** (middle insets)

at 18 and 43 °C, and the corresponding conformation changes of the copolymers on the inner surface of nanochannels (left and right insets).

Then, the temperature gating ratio of **NCS-60** is studied when the glucose concentration is 8.6 g L^{-1} under different pH conditions. When the pH is 4.8 and the glucose concentration is 8.6 g L^{-1}, the ionic current of **NCS-60** decreases with a temperature gating ratio of 0.6 (negative gating behavior), along with the temperature increases from 18 °C to 43 °C (Figure S6A). Then, the temperature gating behaviors of **NCS-60** is studied when the pH changes from 4.8 to 7.4 (Figure S6B). Under this condition, **NCS-60** shows a positive temperature gating behavior with a gating ratio of 1.2, along with the temperature increases from 18 °C to 43 °C. At last, the pH is changed to 10.1, and the ionic current of **NCS-60** increases with a temperature gating ratio of 1.5 (positive gating behavior), along with the temperature increases from 18 °C to 43 °C (Figure S6C). From these experiments, we can find that **NCS-60** has similar gating performances when the glucose concentration is 8.6 g L^{-1} and glucose concentration is 17.2 g L^{-1}.

Reference

(1) Li, P.-F.; Xie, R.; Jiang, J.-C.; Meng, T.; Yang, M.; Ju, X.-J.; Yang, L.; Chu, L.-Y. *J. Membr. Sci.* **2009**, *337*, 310.

(2) Y. Jiang, N. Liu, W. Guo, F. Xia, L. Jiang, *J. Am. Chem. Soc.* **2012**, *134*, 15395-15401.

(3) Xia, F.; Ge, H.; Hou, Y.; Sun, T.; Chen, L.; Zhang, G.; Jiang, L. *Adv. Mater.* **2007**, *19*, 2520.